Cell Reports, Volume *26*

Supplemental Information

p53 Loss in Breast Cancer Leads to Myc Activation, Increased Cell Plasticity, and Expression of a Mitotic Signature with Prognostic Value

Angela Santoro, Thalia Vlachou, Lucilla Luzi, Giorgio Melloni, Luca Mazzarella, Errico D'Elia, Xieraili Aobuli, Cristina Elisabetta Pasi, Linsey Reavie, Paola Bonetti, Simona Punzi, Lucia Casoli, Arianna Sabò, Maria Cristina Moroni, Gaetano Ivan Dellino, Bruno Amati, Francesco Nicassio, Luisa Lanfrancone, and Pier Giuseppe Pelicci

Figure S1

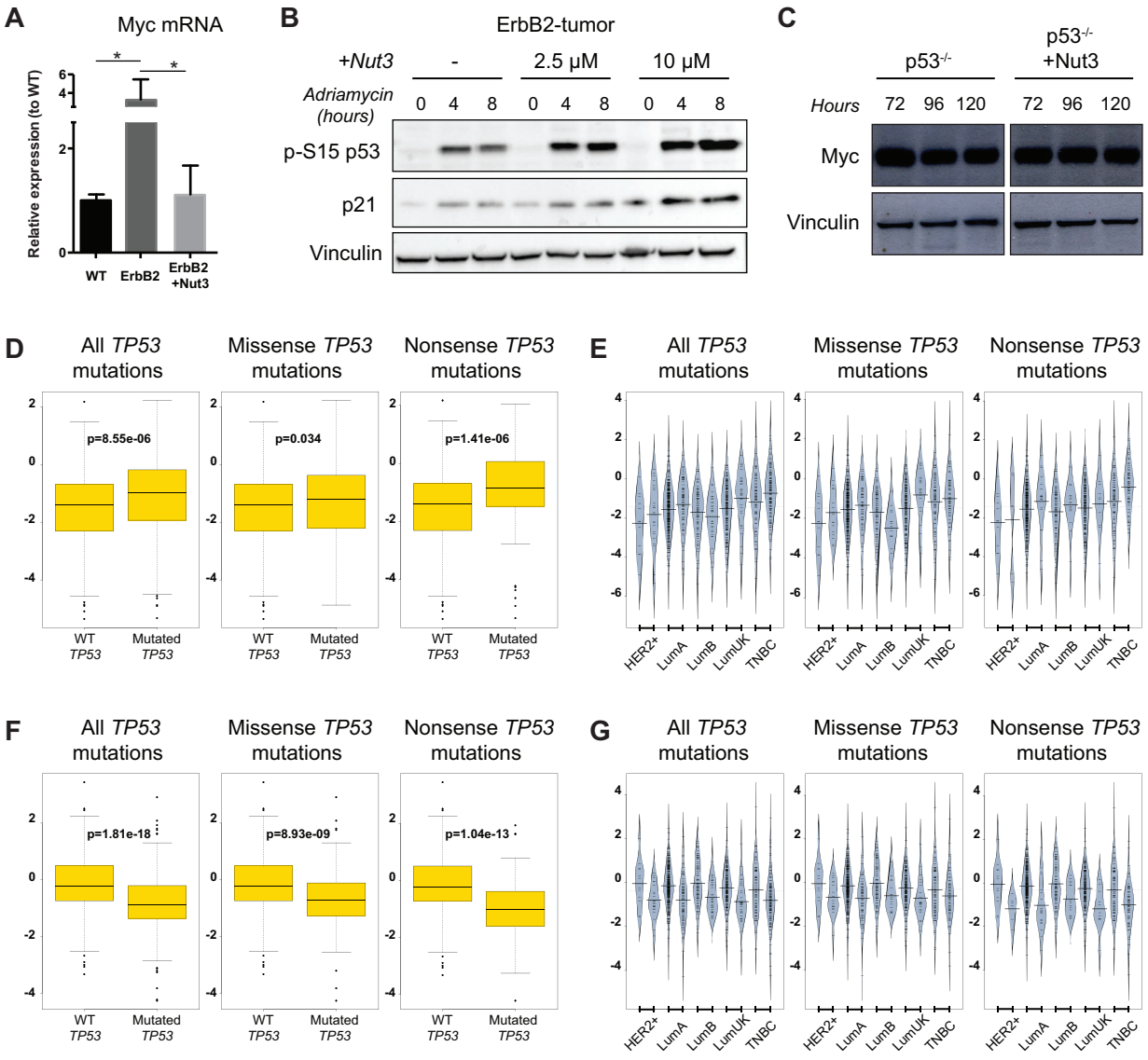

Figure S1. Related to Figure 1. The regulation of Myc expression in ErbB2-tumor cells and human breast cancer samples is p53-dependent. A) RT qPCR of Myc mRNA in WT (n=7) and ErbB2-tumor mammospheres, untreated (n=6) or treated (n=3) with 2.5 µM Nut3, normalized to WT cells. Mean and SD are shown. *p < 0.05. **B)** Western blot of phospho-p53 (p-S15 p53) and p21 expression 4 and 8 h after DNA damage induction (0.5 µM Adriamycin) in ErbB2-tumors, untreated or treated with Nut3 (2.5 and 10 µM). **C)** Western blot of Myc expression in $p53^{-/-}$ cells untreated or treated with Nut3 (2.5 µM) at three selected time points (72, 96 and 120 hours) during mammosphere growth. **D-G)** Analyses of Myc (D-E) and p21 (F-G) RNA levels in TCGA breast cancer samples with WT (n=673) and mutated (n=274) *TP53*. Box plots (D and F) show relative expression levels of all samples carrying any non-synonymous *TP53* mutation (left), only missense mutations (middle) and only nonsense mutations (right), compared to samples with WT *TP53*. Bean plots (E and G) depict relative expression levels of WT versus mutated *TP53* (as in D and F) within each tumor subtype ($HER2^+$; LumA: luminal A; LumB: luminal B; LumUK: luminal unknown; TNBC: triple-negative breast cancer).

Figure S2

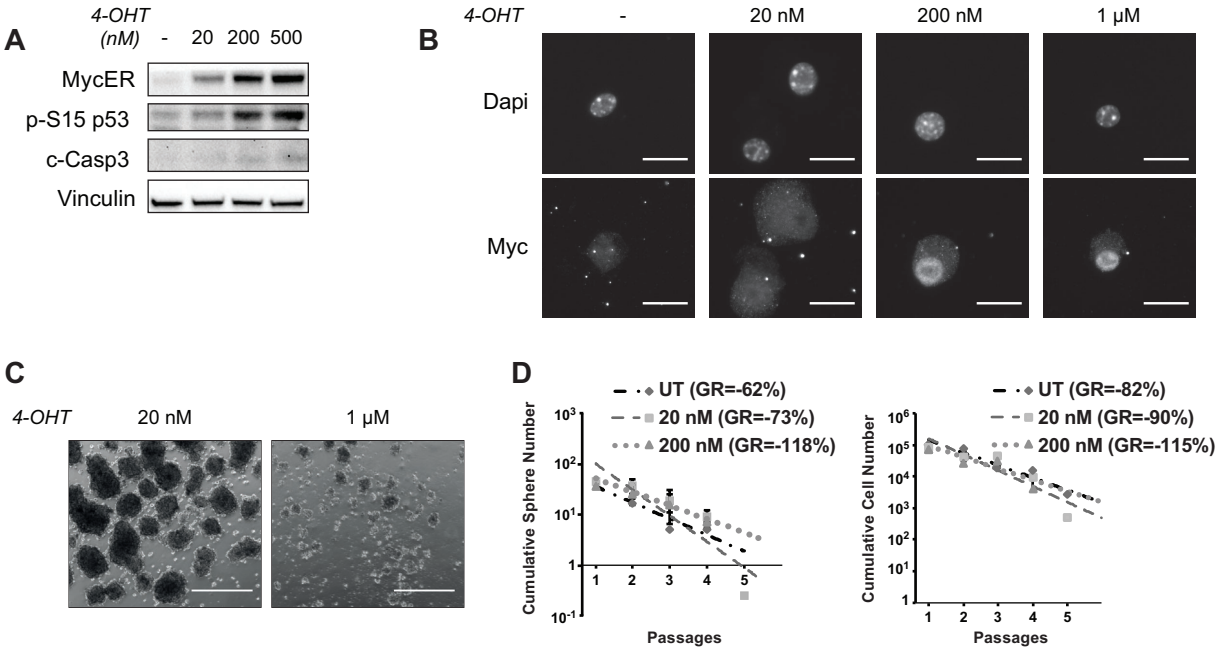

Figure S2. Related to Figure 2. Effects of different doses of 4-OHT on Rosa26-MycER and WT mammospheres. A) Western blot of MycER, phospo-p53 (p-S15 p53) and cleaved-Caspase 3 (c-Casp3) in Rosa26-MycER mammospheres treated with increasing doses of 4-OHT, as indicated. **B)** Immunofluorescence analysis of Myc expression and Dapi staining in Rosa26-MycER mammary cells upon administration of increasing doses of 4-OHT, as indicated. Scale bar, 20 μm. **C)** Representative images of Rosa26-MycER mammospheres treated with 20 nM and 1 μM 4-OHT. Scale bar, 500 μm. **D)** Cumulative sphere and cell number plots of WT mammospheres, untreated (UT) or treated with 20 or 200 nM 4-OHT. Mean and SD of two technical replicates are shown.

Figure S3

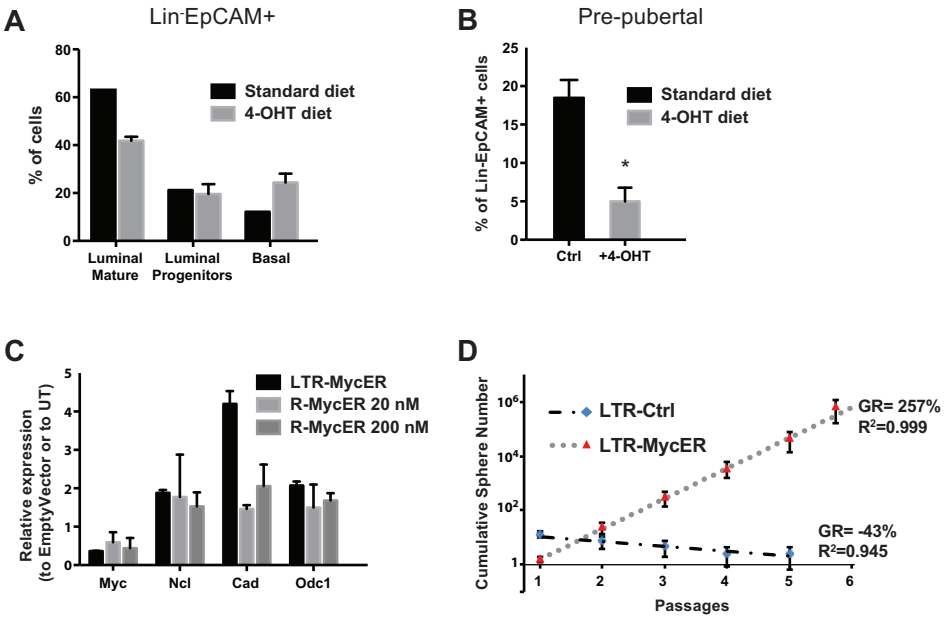

Figure S3. Related to Figure 2. LTR-MycER cells can replace R-MycER cells for *in vivo* studies. **A)** Percentage of Luminal Mature ($CD49f^+CD61^-$), Luminal Progenitor ($CD49f^+CD61^+$) and Basal ($CD49f^+CD61^+$) cells within the Lin^-EpCAM^+ compartment in the mammary glands of 8-week-old WT mice, fed with standard (n=1) or 4-OHT (n=2) diet. Mean and SD are shown. **B)** Percentage of Lin^-EpCAM^+ cells in the mammary glands of 3-week-old WT mice, fed with standard (n=2) or 4-OHT (n=2) diet. Mean and SD are shown. *$p < 0.05$. **C)** RT qPCR of selected transcriptional targets of Myc (c-Myc, Ncl, Cad and Odc1 genes) in LTR-MycER cells (n=1) and R-MycER cells (n=5) treated with 20 or 200 nM 4-OHT; values are expressed as mean fold change relative to the empty vector (for LTR-MycER) or the untreated (for R-MycER) controls, respectively. Error bars represent SD. **D)** Representative cumulative sphere number graph of WT mammospheres transduced with LTR-Ctrl (3 technical replicates) or LTR-MycER (4 technical replicates), without 4-OHT administration. Mean and SD are shown.

Figure S4

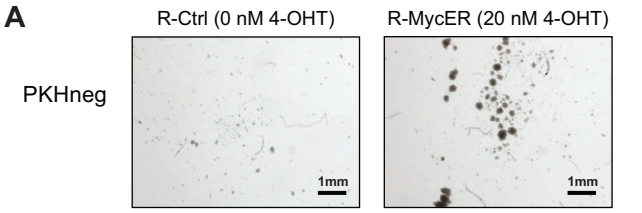

B

Transplants	Mean % Epithelial area	Ki67 index	Hyperplasia/ Dysplasia
WT Ctrl	1.64 ± 1.67	0.44 ± 0.29	+++
PKHneg LTR-MycER	1.95 ± 1.29	0.43 ± 0.29	++

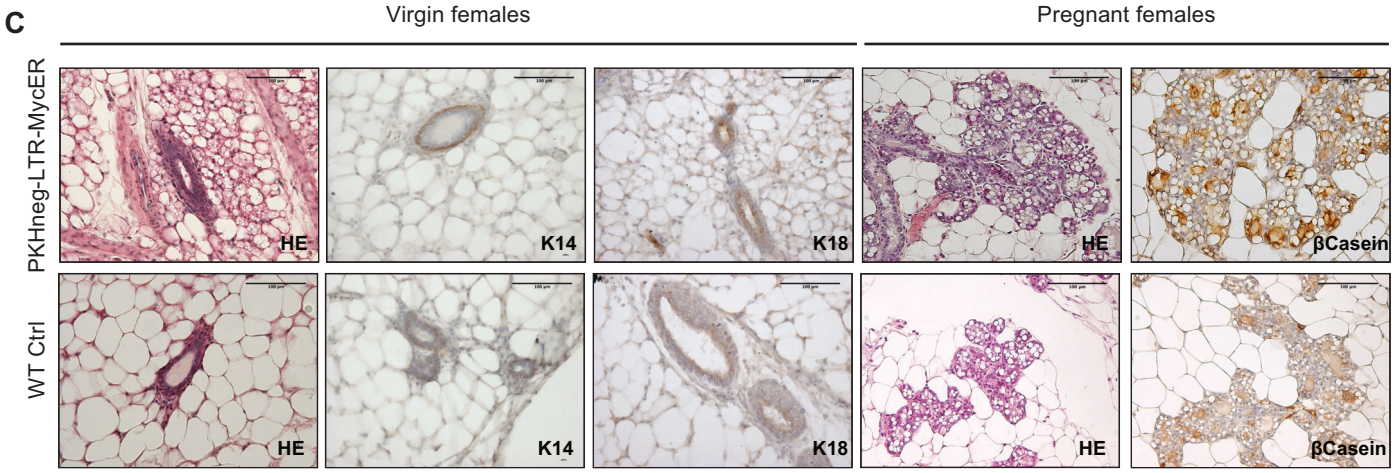

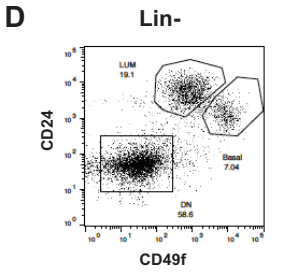

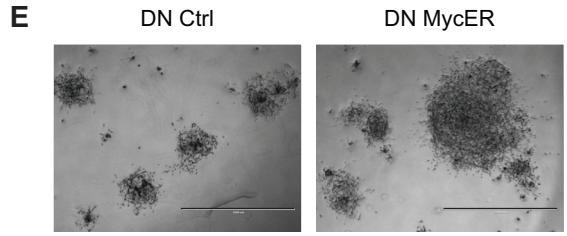

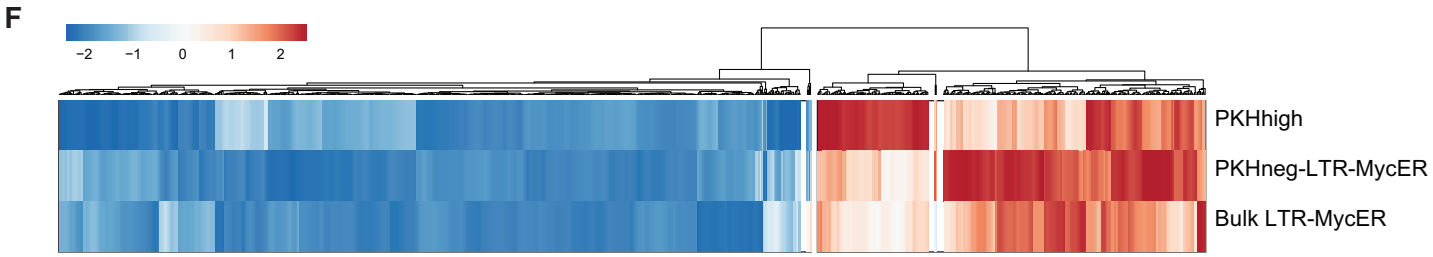

Figure S4. Related to Figure 4. MaProgs are not transformed by constitutive Myc expression. A) Representative images of mammosphere cultures from Rosa26-MycER PKH^{-} progenitors in the absence of 4-OHT (R-Ctrl; left) and upon 1 week of 4-OHT administration (20 nM; R-MycER; right). Scale bar, 1 mm. **B)** Histopathological evaluation of outgrowths (n=6 per group) obtained from the transplantation of 50,000 WT control (Ctrl) or PKH^{-}-LTR-MycER cells. The percentage of the area occupied by mammary epithelium in each examined field (% Epithelial area) and the Ki67 index were calculated by digital image analysis (4 fields per sample). Mean and standard deviation of values in WT Ctrl and PKH^{-}-LTR-MycER outgrowths are shown. Histological grading: (++) = multifocal to diffuse moderate ductal and/or alveolar epithelial hypertrophy and hyperplasia, without relevant cell atypia; (+++) = focal to multifocal areas of mammary epithelial dysplasia with variable cell atypia. Two WT Ctrl samples were excluded from Ki67 calculation and histological grading, given the absence of mammary epithelial structures in the examined sections. **C)** Morphology (hematoxylin-eosin, HE, staining), expression of differentiation markers (basal K14 and luminal K18) and, upon pregnancy (n=5), milk production (β-casein) in the mammary outgrowths derived from PKH^{-}-LTR-MycER cells and their WT Ctrl counterpart. Scale bar, 100 µm. **D)** Representative FACS plot of Lin^{-} primary mammary cells stained with anti-CD24 (PE-conjugated) and anti-CD49f (APC-conjugated) antibodies. **E)** Representative images of organoids originating from double-negative (DN; Lin^{-}CD24^{-}CD49f^{+}) stromal cells, infected with LTR-Ctrl (Ctrl) or LTR-MycER (MycER). Scale bar, 2,000 µm. **F)** Hierarchical clustering of 1,100 genes coherently regulated in PKH^{high} and PKH^{-}-LTR-MycER cells (Table S2), according to the mean expression levels in PKH^{high} cells (n=2), PKH^{-}-LTR-MycER (n=3) and bulk LTR-MycER (n=3) mammospheres, relative to the corresponding values of PKH^{-} cells (n=3).

Figure S5

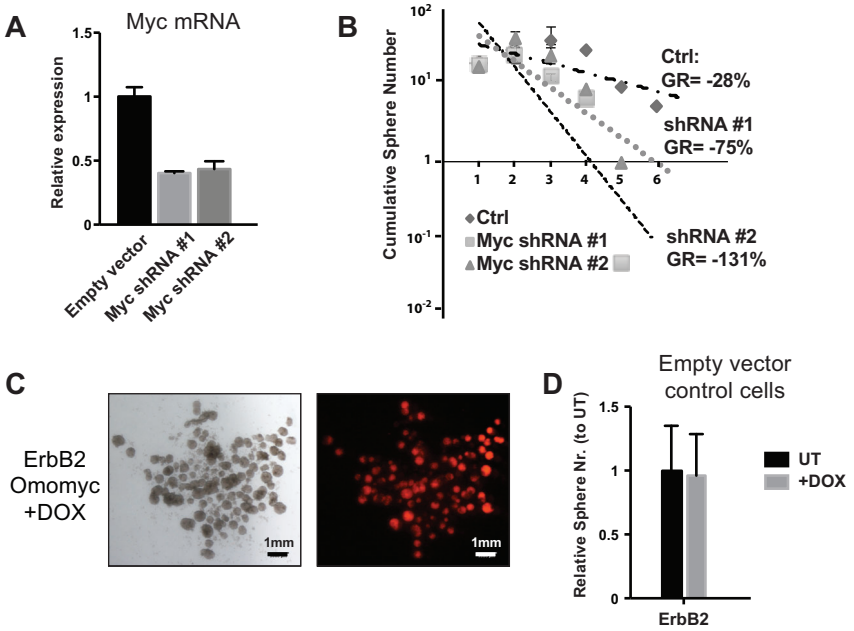

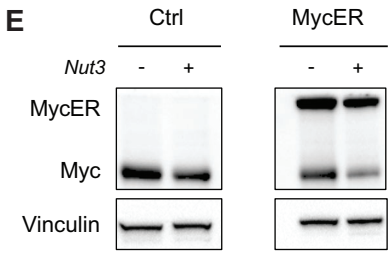

F

Cell Dose	MCF10DCIS.com
10,000	2/2
1,000	5/5
100	4/6
10	4/6
Frequency of repopulating units (95% confidence limit)	**1 / 46.6 (1/114 -1/19.1)**

Figure S5. Related to Figure 5. Myc expression is necessary and sufficient for CSC maintenance and expansion. A) RT qPCR of Myc mRNA in empty vector and shRNA-Myc transduced (Myc shRNA #1 and #2) mammospheres. Results are shown as fold change relative to the empty vector expression (mean and SD of two technical replicates). **B)** Cumulative sphere graph of control (Ctrl) and shRNA-Myc transduced WT mammospheres (Myc shRNA #1 or #2). Mean and SD of two technical replicates are shown. **C)** Doxycycline treatment of Omomyc-transduced mammospheres: representative images of ErbB2-tumor spheres after Doxycycline administration on brightfield (left) or the RFP fluorescent channel (right). Scale bar, 1 mm. **D)** Relative sphere number of ErbB2-tumor (ErbB2; n=2) mammospheres transduced with the TET-inducible empty vector. Spheres were counted at the end of the second passage in the absence (UT) or constant presence of 0.5 μM Doxycycline (+DOX) in the media. Mean and SD are shown. **E)** Western blot analysis of exogenous MycER and endogenous Myc protein levels in ErbB2-tumor cells infected with LTR-Ctrl (Ctrl) or LTR-MycER (MycER), untreated or treated with Nut3 (10 μM) for 16 h. **F)** Limiting dilution transplantation of DCIS cells in the fat pads of NOD/SCID female recipient mice. Tumor initiating cell frequency was calculated by ELDA.

Figure S6

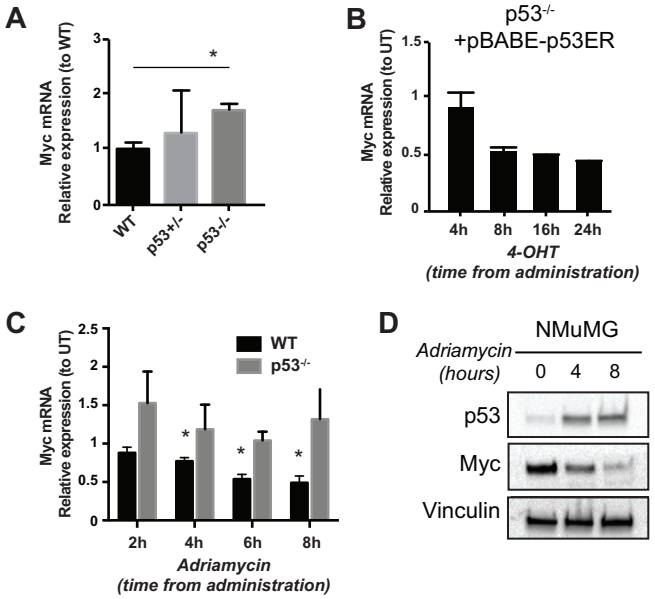

Figure S6. Related to Figure 6. Myc protein and mRNA levels in WT mammary cells are a function of p53 gene dosage and expression. A) Myc levels depend on p53 gene dosage. RT qPCR of Myc mRNA in WT (n=7), $p53^{+/-}$ (n=5) and $p53^{-/-}$ (n=2), normalized to WT. Mean and SD are shown. *$p < 0.05$. **B)** Myc levels depend on p53 expression. RT qPCR of Myc mRNA in $p53^{-/-}$ mammospheres transduced with the inducible p53ER vector and treated with 4-OHT (200 nM) for the indicated times, normalized to time=0. Mean and SD of two technical replicates are shown. **C)** DNA damage induces p53-dependent Myc mRNA downregulation in mammospheres. RT qPCR of Myc mRNA in WT (n=3) and $p53^{-/-}$ (n=2) mammospheres. Results are shown as fold change relative to the untreated samples. Mean and SD are shown. *$p < 0.05$. **D)** Western blot analysis of p53 and Myc expression in NMuMG cells treated with 0.5 μM Adriamycin (at 0, 4 and 8 h).

Figure S7

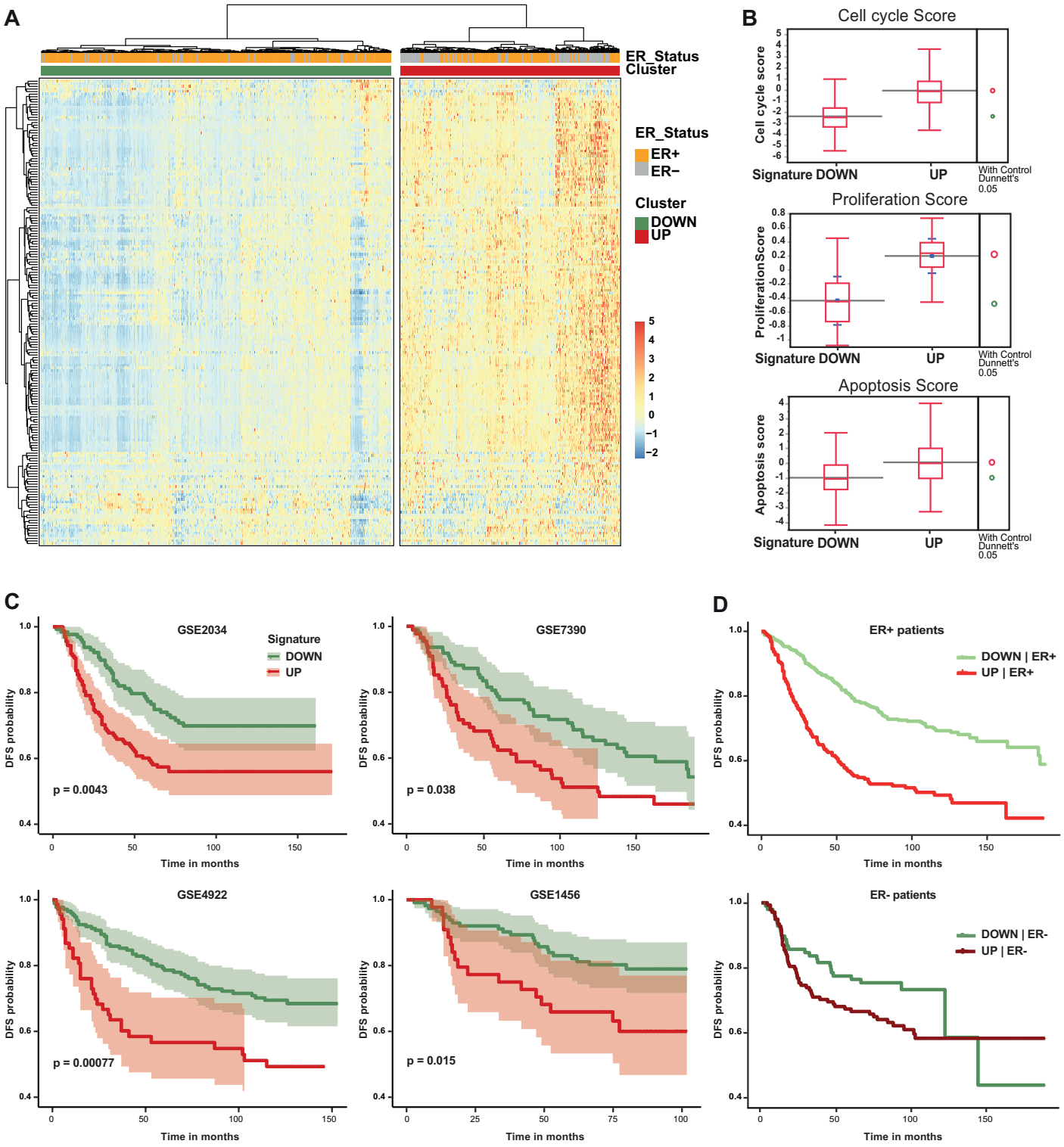

Figure S7. Related to Figure 7. Patient stratification and survival analyses according to the MitSig expression. A) Hierarchical clustering of 1032 TCGA primary breast cancer patients according to the expression levels of the MitSig genes (values are expressed as Z-score). Color code of ER status and Z-score scale defined in the legend on the right. **B)** Box plots depict average RPPA score of Cell-cycle, Proliferation and Apoptosis pathways (Akbani et al., 2014) in "DOWN" and "UP" cohorts. Red circles mark significant differences between the two groups (non-parametric Dunnet's test, $p < 0.05$). **C)** Disease-free survival (DFS) curve of each study (GSE2034, GSE4922, GSE7390, GSE1456) individually. Logrank test p-values as indicated. **D)** DFS curve of ER positive (upper panel) and ER negative (lower panel) breast cancer patients grouped in "DOWN" and "UP" cohorts. Wald test p-value on MitSig effect inside an ER status adjusted Cox model 1.58e-08.

Table S4

Related to Figure 7. Number of participants and corresponidng clinal information reported in datasets GSE1456, GSE2034, GSE4922 and GSE7390

	GSE1456	GSE2034	GSE4922	GSE7390	Total
Participants	159	286	249	198	892
Status_Relapse	X	X	X	X	892
Time_Relapse	X	X	X	X	892
Subtype	X				159
ER_status	X	X	X	X	892
Grade	X		X	X	606
Lymph_Node_status			X	X	447
P53_status			X		249
Age			X	X	447
Tumor_size			X	X	447